JOURNAL OF CATALYSIS 95, 227–243 (1985)

Methanol and Methane Formation over Palladium/Rare Earth Oxide Catalysts

CHAKKA SUDHAKAR AND M. ALBERT VANNICE[1]

Department of Chemical Engineering, Pennsylvania State University, University Park, Pennsylvania 16802

Received January 15, 1985; revised April 30, 1985

Lanthanide rare earth oxide (REO)-supported Pd systems can provide very good CO hydrogenation catalysts, especially for CH_3OH formation. At low temperature and 1 atm, the major product was methanol but the selectivity shifted to methane at higher temperatures because of equilibrium constraints. The turnover frequency (TOF) values for CH_4 varied more than tenfold, but all, except for Pd/Eu_2O_3, were more than an order of magnitude higher on these catalysts than on Pd/SiO_2 or pure Pd metal. Activation energies for CH_4 on these Pd/REO samples were consistently near 32 kcal/mole and very close to the value on Pd powder, indicating that the methanation reaction mechanism may be similar on all these catalysts. At 14.6 atm total pressure, the major product over the Pd/REO catalysts was methanol, and the selectivity for oxygenates ranged from 78 to 96% at 225°C. Activation energies for CH_3OH varied from 17 to 21 kcal/mole and were close to the value obtained for Pd powder. Pd/La_2O_3 and Pd/Nd_2O_3 were the most active CH_3OH catalysts whereas Pd/CeO_2 was the least active. All the Pd/REO catalysts deactivated initially at high pressure but reached steady state after about 30 hr on stream, with the stabilized activity being approximately half the initial activity in all cases. In contrast, the activity of Pd powder increased with time before reaching a steady state. The selectivity of Pd powder for oxygenates was lower compared to REO-supported Pd, and the CH_3OH TOF over Pd powder was an order of magnitude lower than the least active Pd/REO catalyst. The role of these supports in CH_3OH synthesis is consistent with that of promoting the concentration of formyl/formate intermediates on the surface, particularly at the Pd–support interface.

INTRODUCTION

In the conversion of syngas to hydrocarbons or oxygenates, it is desirable to produce only the most valuable chemicals from syngas due to its high cost, and oxygenates are one of the most important groups of compounds. The production of methanol has gained importance after the development of the Mobil process to convert methanol to gasoline (*1*). In addition, methanol has several other uses such as an industrial solvent, a raw material for the production of different chemicals, and now it is being used to blend with gasoline (*2*). With slight engine modifications, automobiles can run on pure methanol, which is a much cleaner fuel than gasoline, and for this reason it is predicted that methanol production will increase steeply in the coming years (*2*).

Industrial methanol synthesis catalysts consist of mixed oxides of ZnO and Cr_2O_3 in the older high-pressure process or are based on Cu in combination with various oxides such as ZnO, Cr_2O_3, Al_2O_3 in the newer low-pressure synthesis process (*3*, *4*). In 1978 Poutsma *et al.* (*5*) reported that very selective methanol synthesis could be achieved under thermodynamically favorable reaction conditions over Pd, Pt, or Ir supported on silica, and that palladium was at least an order of magnitude more active than Pt or Ir. This report initiated much interest in the possibility that Pd-based catalysts for methanol synthesis (*6–16*) might provide an alternative to Cu-based catalysts, which are easily susceptible to sulfur poisoning (*3*). Published data show that the

[1] To whom correspondence should be sent.

0021-9517/85 $3.00

activity and selectivity of Pd catalysts are dependent on the support used to disperse Pd. Initially, it was thought that mildly basic supports such as MgO and La_2O_3 favor methanol formation, whereas strongly acidic or strongly basic supports such as Al_2O_3, TiO_2, or Li_2O inhibit methanol formation (*15*); however, although this trend has generally been observed, no universal agreement has been reached on the influence of the support on selectivity to methanol over Pd.

The present investigation, which deals with the CO hydrogenation reaction over Pd dispersed on rare earth oxide (REO) supports, was initiated for several reasons. First, it is already known that La_2O_3 and Nd_2O_3 are two of the best supports for methanol formation over Pd (*7, 9, 12*). Second, only one systematic study of the use of these oxides as catalyst supports has been made, which showed that they play an important role in determining the catalytic properties of Pd (*17*). Third, the influence of smoothly varying periodic trends in surface basicity and cationic 4*f*-electron configuration on catalytic properties in the methanol synthesis reaction could be studied. Finally, the results obtained from this study should enhance the understanding of the mechanism of methanol and methane formation on supported Pd catalysts.

Pd was dispersed on the first half of the lanthanide oxides, namely, La_2O_3, CeO_2, Pr_6O_{11}, Nd_2O_3, Sm_2O_3, Eu_2O_3, and Gd_2O_3, using a nonaqueous method to prevent the hydrolysis of the oxide surface (*18*). These catalysts were thoroughly characterized using a variety of techniques and were then used in this study.

EXPERIMENTAL METHODS

Materials

The rare earth oxide (REO) support materials used in this investigation were lanthanum oxide, La_2O_3, 99.9% from Molycorp. Inc., along with cerium oxide, CeO_2, 99.9%; praseodymium oxide, Pr_6O_{11}, 99.9%; neodymium oxide, Nd_2O_3, 99.9%; samarium oxide, Sm_2O_3, 99.9%; europium oxide, Eu_2O_3, 99.9%; and gadolinium oxide, Gd_2O_3, 99.9% from the Sigma Chemical Company. The procedure used to increase their surface areas and the BET surface areas of these treated supports have been reported elsewhere (*18*). Palladium powder, Puratronic grade (99.998%) was obtained from Johnson Matthey Inc. The only impurities reported were Si (2 ppm), Fe (1 ppm), and Ca, Cu, Ag (<1 ppm each). Diamminepalladium(II) nitrite, $Pd(NH_3)_2(NO_2)_2$, was obtained from Alfa Products (Ventron Corp.), and *N,N*-dimethylformamide, $HCON(CH_3)_2$ (DMF), was Spectra ACS grade from the Eastman Kodak Company.

The gases used in the chemisorption and kinetic studies—H_2 (MG Scientific, 99.999%), CO (Matheson, 99.99%), and He (MG Scientific, 99.9999%)—were further purified before use. H_2 was passed through a Deoxo unit (Engelhard Ind.), a 5A molecular sieve trap, and an Oxy-trap (Alltech Associates). The He was passed through a Drierite-molecular sieve gas purifier (Alltech Associates) followed by an Oxy-trap. CO was further purified by passage through a 5A molecular sieve trap maintained at 150°C to remove water and carbonyls. Both H_2 and He were supplied when needed to the chemisorption system through external lines, whereas CO was stored in 5-liter glass bulbs attached to it. The air for calcination was obtained from MG Scientific (zero grade) and was used without any purification.

Catalyst Preparation

Catalysts containing a nominal 1.5% Pd by weight were prepared using the Pd complex $Pd(NH_3)_2(NO_2)_2$ dissolved in DMF along with a multiple incipient wetness method (*18*). They were dried overnight at 120°C in air and later calcined in flowing air (450 cm^3/min) in a tubular furnace at 500°C for 2 hr prior to their use. The Pd loadings in these Pd/REO catalysts were determined by plasma emission spectroscopy using a

Spectraspan IIIA emission spectrometer. The detailed procedure for this has been reported elsewhere (*18*).

X-Ray Diffraction (XRD)

A Philips XRG-3000 X-ray diffractometer equipped with an APD 3600 computer containing all the ASTM files in memory was used for the XRD experiments. Cu$K\alpha$ radiation was used and the samples were scanned in the 2θ range of 10° to 60°. The Scherrer equation with Warren's correction for instrumental line broadening, which was found to be 0.24° at a 2θ value of 40°, was used to analyze the Pd(111) peak for the metal crystallite size calculations.

Adsorption Measurements

A glass high-vacuum system, which consisted of an Edwards Model EO2 oil diffusion pump with liquid-nitrogen traps located on either side, was used to study the chemisorption of H_2 and CO on these Pd catalysts and also to measure the BET surface areas of the supports and the Pd powder. An ultimate vacuum below 10^{-4} Pa could be reached in the system. A Texas Instruments Model 145 precision pressure gage was used to measure the gas pressures during isotherm measurements. Details have been given elsewhere (*19*).

The sequence of adsorption experiments for both fresh catalysts and those used in the kinetic studies was as follows: (i) reduce in flowing H_2 (50 cm^3/min) at 300°C for 1 hr, (ii) evacuate at 275°C for 30 min, (iii) adsorb H_2 at room temperature, (iv) evacuate at room temperature for 30 min, (v) readsorb H_2, (vi) heat in flowing H_2 (50 cm^3/min) at 300°C for 30 min, (vii) evacuate at 275°C for 30 min, (viii) determine first CO isotherm at room temperature, (ix) evacuate at room temperature for 5 min, (x) determine second CO isotherm. In the case of Pd powder, the sequence used was as follows: (i) heat in flowing He (50 cm^3/min) at 250°C for 1 hr, (ii) cool to room temperature, evacuate, and measure BET surface area, (iii) heat in flowing H_2 (50 cm^3/min) at 350°C for 1 hr, (iv) evacuate at 300°C for 1 hr, (v) measure first CO isotherm at room temperature, (vi) evacuate at room temperature for 5 min, (vii) measure second CO isotherm. H_2 chemisorption was not measured in the case of Pd powder due to the large amount of H_2 absorption into the Pd crystallites.

The amount of H_2 chemisorbed on the surface of Pd, as well as that absorbed to form the bulk β-hydride phase, was measured by using the method of Benson *et al.* (*20*). This method involves the measurement of two isotherms, the first of which consists of both adsorbed and absorbed hydrogen, and the second which represents the hydrogen absorbed in the bulk. The difference at 250 Torr was taken as the chemisorbed hydrogen on Pd, and by extrapolating the second isotherm to zero pressure the amount of H_2 absorbed in bulk Pd was obtained. The bulk hydride ratio should typically be near 0.6 (*20*). The irreversibly adsorbed CO was determined using the method of Yates and Sinfelt (*21*).

Pd crystallite sizes of fresh, as well as used, catalyst samples were calculated using the equation

$$\bar{d}_s(\text{nm}) = \frac{1.13}{D},$$

where d_s is the surface-weighted average crystallite diameter, and D is the dispersion (fraction exposed) of Pd (*22*).

Transmission Electron Microscopy (TEM)

A Philips EM 300 transmission electron microscope was used to take TEM micrographs of the catalyst samples at an acceleration voltage of 80–100 kV and a 20 μm objective aperture. The catalyst samples were ground to a fine powder between two glass slides and ultrasonically dispersed in toluene. A drop of this solution was placed on a 400-mesh copper grid which was coated with Formvar and carbon films, the solvent was evaporated at room tempera-

ture in air, and then was examined in the microscope. Typical magnifications ranged from 132,800 to 200,000 and the Pd particle diameters were measured using a calibrated magnifying eyepiece after enlarging the pictures 2.6 times.

Kinetic Measurements

All the kinetic studies were performed in a steady-state, plug-flow microreactor which was made of 316 stainless steel and whose inner surface was Alonized to make it nonreactive, and the remainder of the reaction system was made of 316 stainless steel. It was equipped with Brooks mass flow controllers and the pressure in the system was controlled by a stainless-steel, dome-loaded, back-pressure regulator (BPR) (Circle Seal Corp.). The pressure was monitored by a pressure transducer with digital readout (Validyne Corp.). The BPR and the transfer lines from the reactor to the sampling system were kept heated at about 105°C by means of heating tapes. A fluidized sandbath (Techne Corp.) was used to heat the reactor, and a thermocouple probe attached to the reactor very close to the catalyst bed measured the temperature of the catalyst. Further details of the system will be published elsewhere (*23*).

The effluent gas was analyzed for CO, CH_4, CO_2, C_2H_4, C_2H_6, H_2O, CH_3OH, and dimethyl ether (DME) using a Perkin–Elmer Sigma 2B gas chromatograph equipped with a heated sampling valve and a thermal conductivity detector. A 2 mm × 2.2 m Chromosorb 106 column, temperature-programmed from 45 to 150°C, was used to separate the various constituents of the effluent gas. A Hewlett–Packard 3390 integrator or a Perkin–Elmer LCI 100 integrator was used to determine peak areas and compositions.

The amount of catalyst used in the reaction varied between 0.4 and 0.7 g and, using an H_2/CO ratio of 3, the total flow rate was either 24 or 48 cm^3 (STP) · min^{-1}. In the case of Pd powder, 2 g of catalyst (40–80 mesh) was used in the reaction because of its low activity. The CO conversions were kept below 5% to eliminate heat and mass transfer effects, and a temperature bracketing technique, alternating between pure H_2 and H_2/CO mixtures, was used when the reaction was conducted at 1 atm (*22*). At high pressure, 45 min between each point was found to be sufficient to achieve stable conditions. At both 1 and 14.6 atm (200 psig), activity data were obtained during ascending and descending temperature sequences to check for deactivation.

For the Pd/REO catalysts a fresh sample was always used in the reaction, whereas the Pd powder was used after characterization by BET and CO adsorption measurements. After loading the catalyst in the reactor, it was reduced in flowing H_2 (50 cm^3/min) at 300°C for 1 hr (350°C in the case of Pd powder to facilitate reduction of the large crystallites) before starting the CO hydrogenation reaction. After the completion of the runs at low pressure, the catalyst was reduced again in flowing H_2 (50 cm^3/min) at 300°C for 1 hr (350°C in the case of Pd powder), cooled to the reaction temperature, pressurized with pure H_2 to 14.6 atm and, after stabilizing for about 20 min, the CO flow was initiated. The activity on-stream was usually monitored for 48 hr after which time the catalysts reached steady state, then Arrhenius plots were obtained between 200 and 260°C.

RESULTS

Catalyst Characterization

The chemisorption behavior of the fresh Pd/REO catalysts and the Pd powder are presented in Table 1, which presents the chemisorption uptakes of H_2 and CO and the Pd dispersions calculated assuming adsorption ratios of $H_a/Pd_s = CO_a/Pd_s = 1$. Also presented are the amounts of hydrogen absorbed (H_b) to form the bulk β-hydride, the hydride ratio H_b/Pd_b, where Pd_b is the amount of bulk Pd (total Pd − Pd_s), and the ratio of chemisorbed CO molecules to H atoms. Table 2 presents the same ad-

TABLE 1

Chemisorption Behavior of Fresh Pd/REO Catalysts Reduced at 300°C

Catalyst	Chemisorption (μmole g^{-1})		% Dispersion, based on		H_b[a] (μmole g^{-1})	H_b/Pd_b[a]	CO_a/H_a	Support surface area (m^2 g^{-1})
	H_2	CO	H_2	CO				
1.50% Pd/La_2O_3	14.7	37.3	20.8	26.4	20.5	0.37	1.27	28.5
1.60% Pd/CeO_2	5.2	11.8	6.9	7.9	41.5	0.59	1.15	5.3
1.60% Pd/Pr_6O_{11}	13.7	18.0	18.2	12.0	34.2	0.56	0.66	9.6
1.55% Pd/Nd_2O_3	19.4	27.5	26.6	18.9	24.6	0.46	0.71	15.0
1.52% Pd/Sm_2O_3	24.0	54.7	33.5	38.2	26.2	0.55	1.14	13.0
1.66% Pd/Eu_2O_3	22.3	48.8	28.6	31.3	30.4	0.55	1.09	13.4
1.67% Pd/Gd_2O_3	15.0	32.7	19.1	20.8	33.7	0.53	1.09	7.0
Pd Powder[b]	—	4.2	—	0.045	—	—	—	—

[a] H_b is hydrogen in bulk Pd, Pd_b is the bulk Pd.
[b] Reduced at 350°C.

sorption results for the Pd/REO catalyst after use in the CO hydrogenation reaction. The used Pd powder was not characterized.

The following conclusions can be drawn from Table 1. [1] The dispersion of Pd based on the H_2 chemisorption varies from 6.9% in the case of Pd/CeO_2 to 33.5% for Pd/Sm_2O_3; however, the low value for Pd/CeO_2 is likely due to the low surface area of the CeO_2 used (~5 m^2 g^{-1}). A similar range exists when based on CO adsorption. [2] The hydride ratio for the β-phase hydride in all the catalysts is consistently between 0.5 to 0.6 indicating well-behaved Pd particles. This result indicates the absence of complete encapsulation of some of the Pd particles by the support. Only in the case of Pd/La_2O_3 is the value significantly lower than 0.55. [3] The ratio of adsorbed CO to adsorbed H atoms, CO_a/H_a, is typically close to unity, indicating a consistent surface stoichiometry on most of these Pd crystallites. On the fresh Pd/Pr_6O_{11} and Pd/Nd_2O_3 samples the CO_a/H_a ratios are significantly lower which may indicate more bridge-bonded CO on these catalysts. In the cases

TABLE 2

Chemisorption On Used Pd/REO Catalysts Reduced at 300°C

Catalyst	Chemisorption (μmole g^{-1})		% Dispersion, based on		H_b (μmole g^{-1})	H_b/Pd_b[a]	CO_a/H_a	$\frac{H_a \text{ (fresh)}}{H_a \text{ (used)}}$
	H_2	CO	H_2	CO				
1.50% Pd/La_2O_3	4.2	11.3	5.9	8.0	32.5	0.49	1.35	3.5
1.60% Pd/CeO_2	4.2	7.1	5.5	4.7	40.2	0.57	0.85	1.2
1.60% Pd/Pr_6O_{11}	5.4	8.6	7.1	5.7	38.3	0.55	0.80	2.6
1.55% Pd/Nd_2O_3	3.0	7.6	4.1	5.2	35.6	0.51	1.3	6.5
1.52% Pd/Sm_2O_3	8.2	15.8	11.4	11.0	33.6	0.53	0.95	2.9
1.66% Pd/Eu_2O_3	9.1	16.4	11.7	10.5	35.8	0.52	0.90	2.4
1.67% Pd/Gd_2O_3	6.1	12.0	7.7	7.6	40.3	0.56	1.0	2.5

[a] Pd_b = bulk Pd atoms.

TABLE 3

Pd Crystallite Sizes of Pd/REO Catalysts after Use in the CO Hydrogenation Reaction (at 1 atm)

Catalyst	Pd crystallite size (nm) from			TEM[a]	
	H_2 chemisorption	CO chemisorption	XRD [Pd(111)]	SWA	VWA
1.50% Pd/La_2O_3[b]	19	14	17	13	14
1.60% Pd/CeO_2	20	24	17	16	24
1.60% Pd/Pr_6O_{11}	16	20	19	14	20
1.55% Pd/Nd_2O_3	28	22	17	—	—
1.52% Pd/Sm_2O_3	10	10	16	14	16
1.66% Pd/Eu_2O_3	10	11	15	—	—
1.67% Pd/Gd_2O_3	15	15	15	—	—

[a] Not much accuracy is claimed for these values since the number of particles counted was small (50–100). SWA, surface-weighted average; VWA, volume-weighed average.

[b] Pd particles not clearly identifiable.

where the ratio is noticeably higher than 1, it might be attributed to the creation of special sites for CO chemisorption in the Pd–support interface region. For this reason, we prefer the dispersion measurements based on H_2 chemisorption to those based on CO chemisorption. It should be noted that the pure support materials do not chemisorb either H_2 or CO after H_2 reduction at 300°C (*17*).

By comparing Tables 1 and 2 it can be seen that after using these catalysts in the CO hydrogenation reaction, the available Pd surface area decreased significantly, but to different extents with different catalysts. The greatest decrease occurred with Pd/Nd_2O_3 (a factor of 6.5), whereas the smallest decrease occurred in the case of Pd/CeO_2 (a factor of 1.2). In all the other cases, the ratios were similar, varying between 2.4 and 3.5. The hydride ratios for all the used catalysts were close to 0.55, again indicating normal behavior for these larger particles, and the CO_a/H_a chemisorption ratios are again near unity for all the catalysts. Only Pd/Nd_2O_3 showed a significant change in the ratio from the fresh to the used sample.

The Pd particle sizes in the fresh catalysts, calculated from H_2 and CO chemisorption, XRD, and TEM techniques, were reported in a previous paper (*18*). Pd/CeO_2 was the only catalyst which showed a Pd(111) peak in the XRD pattern, and the Pd particle size calculated from this peak was in reasonable agreement with that calculated from chemisorption, whereas TEM showed Pd particles of much smaller size than those indicated by the other two techniques. No Pd particles were visible by TEM for the Pd/La_2O_3 catalysts, but in the other cases the particle sizes from TEM agreed reasonably well with those calculated from chemisorption measurements.

Table 3 presents the Pd crystallite sizes of the Pd/REO catalysts after their use for CO hydrogenation at 1 atm. Unlike the fresh catalysts, all the used catalysts showed weak Pd(111) peaks. It should be mentioned that the Pd particle sizes calculated from the XRD measurements are only approximate because of the error involved in the measurement of these low intensity peaks. From the table, it can be seen that there is quite reasonable agreement between the Pd crystallite sizes calculated from the H_2 and CO chemisorption and from the XRD measurements. It can also be concluded from Table 3 that the surface-weighted and volume-weighted average Pd crystallite sizes calculated by TEM are in reasonable agreement with the values ob-

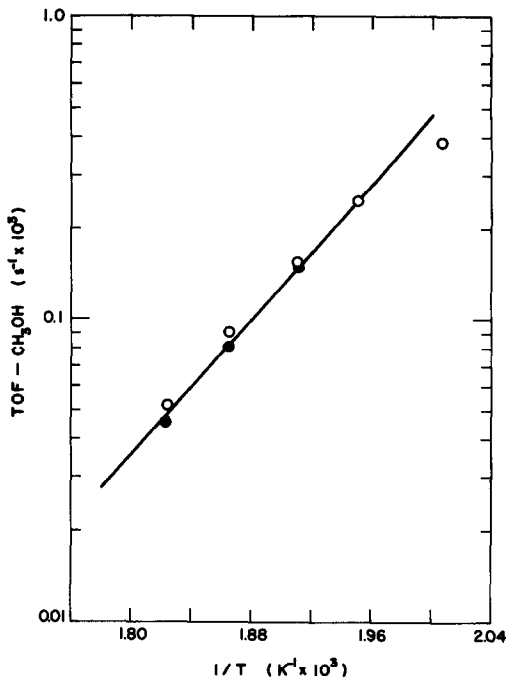

FIG. 1. Temperature dependence of methanol formation at 1 atm over 1.67% Pd/Gd_2O_3. Increasing T (○); decreasing T (●).

tained from chemisorption and XRD, respectively, and all indicate Pd crystallites in the range of 10–20 nm.

Catalytic Studies

The higher pressure reaction was conducted at 14.6 atm at either 225 or 250°C, depending on the activity of the catalyst. At 1 atm pressure, the major products were CH_4, CO_2, and CH_3OH for all the Pd/REO catalysts. Over the Pd powder ethane was produced in significant amounts but no methanol or DME was detected over pure Pd powder above 250°C, and the activity was too low to use lower temperatures. At 1 atm the CH_3OH and DME formation decreased with increasing temperature, indicating that their formation was equilibrium limited. When the rate of CH_3OH formation was plotted against $1/T$, the resultant plots were found to be straight lines, such as that for Pd/Gd_2O_3 shown in Fig. 1, whose slopes gave ΔH values near −24 kcal/mole, in good agreement with the enthalpy of formation for CH_3OH (−23 kcal/mole at 225°C).

The Arrhenius plots of CH_4 formation over all the catalysts at 1 atm pressure were straight lines and showed little or no deactivation; however, CO_2 formation was found to be more complicated. For Pd/La_2O_3, Pd/CeO_2, Pd/Pr_6O_{11}, Pd/Nd_2O_3, and Pd powder, the Arrhenius plots for CO_2 formation were straight lines; but on Pd/Sm_2O_3, Pd/Eu_2O_3, and Pd/Gd_2O_3, they were made up of two straight lines intersecting at about 260°C for Pd/Eu_2O_3 and Pd/Gd_2O_3, and at 240°C for Pd/Sm_2O_3. One of the latter Arrhenius plots is shown in Fig. 2. This behavior is difficult to explain, but it may be connected with the low-temperature decomposition of RE carbonates which were formed by exposure to CO_2 in the air during impregnation (*47*).

The catalytic properties of Pd/REO catalysts and of Pd powder in the CO hydrogenation reaction at 1 atm pressure are pre-

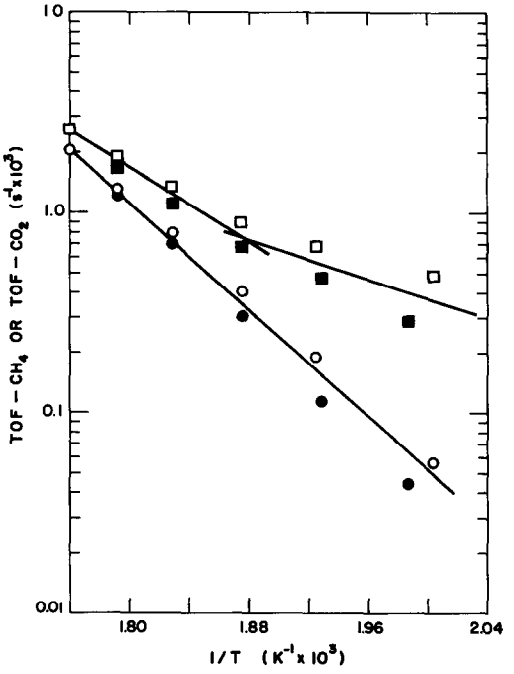

FIG. 2. Temperature dependence of CH_4 (○) and CO_2 (□) formation at 1 atm over 1.66% Pd/Eu_2O_3 (H_2/CO = 3). Open symbols, increasing T; filled symbols, decreasing T.

TABLE 4

Kinetic Behavior of Pd Catalysts for CO Hydrogenation (1 atm, $H_2/CO = 3$)

Catalyst	Activity at 275°C (μmole · $s^{-1} \cdot g^{-1} \times 10^3$)		Turnover frequency[a] ($s^{-1} \times 10^3$)			E_a (kcal/mole)		Comments on oxygenate formation (methanol and dimethyl ether) R = rate CH_3OH/rate CH_4
			CH_4		CO_2 at 275°C	CH_4	CO_2	
	CH_4	CO_2	250°C	275°C				
1.50% Pd/La_2O_3	87	112	0.68	3.0	3.8	33.7	16.4	Much CH_2OH, little DME formed $R_{225°C} = 1.3$
1.60% Pd/CeO_2	80	42	2.0	7.8	4.0	31.2	27.9	Little CH_3OH formed $R_{225°C} = 0.5$
1.60% Pd/Pr_6O_{11}	94	98	0.84	3.4	3.6	31.9	22.4	Much CH_3OH, little DME formed $R_{225°C} \approx 0.5$–1
1.55% Pd/Nd_2O_3	122	166	0.81	3.2	4.3	31.2	18.1	CH_3OH formed, analysis not quantitative
1.52% Pd/Sm_2O_3	130	145	0.66	2.7	3.0	32.1	24.1 (11.9)[b]	Much CH_3OH, little DME $R_{225°C} = 1.6$; $R_{212°C} = 4.7$
1.66% Pd/Eu_2O_3	34.4	58	0.19	0.8	1.3	31.8	20.7 (11.7)[b]	Much CH_3OH, little DME $R_{225°C} = 2.8$
1.67% Pd/Gd_2O_3	90	92	0.70	2.9	3.1	32.4	28.1 (19.0)[b]	Much CH_3OH, little DME $R_{225°C} = 2.6$
Pd powder	0.5	0.03	0.03	0.12	0.06	31.7	16.1	No CH_3OH, no DME at 250°C (activity too low at 225°C)

[a] Based on H_2 chemisorption on the fresh sample.
[b] Low-temperature region of the Arrhenius plot.

sented in Table 4. Activities at 275°C are listed as well as turnover frequencies calculated using the H_2 chemisorption values on the fresh catalyst because this series of runs was the first conducted. The CO chemisorption value was used in the case of Pd powder. The pure REO supports were found to be inactive in this reaction under the experimental conditions used in this work (*17*). It can be seen from Table 4 that the methane TOF varies between 0.8×10^{-3} s^{-1} for Pd/Eu_2O_3 and 7.8×10^{-3} s^{-1} for Pd/CeO_2; however, most values are near those reported for Pd/Al_2O_3 and Pd/SiO_2–Al_2O_3 catalysts (*22a*). The CO_2 TOF values are typically near $3 \pm 1 \times 10^{-3}$ s^{-1}. These results show that there appears to be a mild support effect for CO hydrogenation on these Pd/REO catalysts at low pressure consistent with a previous study (*17*). The TOF_{CH_4} and TOF_{CO_2} values are 0.12×10^{-3} and 0.06×10^{-3} s^{-1}, respectively, for the Pd powder, which are very low compared to those for the Pd/REO catalysts. It is interesting to note that the CH_4 TOF obtained for Pd powder in this study is the same as that obtained for Pd/SiO_2 catalysts by Wang *et al.* (*22a*). This is in agreement with results for Pt, reported in a recent study, that the CH_4 TOF on high-purity Pt powder is the same as that on Pt/SiO_2 (*24*). Both sets of results indicate that there is no apparent support effect of SiO_2 on Pd and Pt in the methanation reaction. However, it is noteworthy that dispersing Pd on most supports, except SiO_2, produces a marked enhancement in the specific activity.

Another very interesting observation that can be made from Table 4 is that the E_a values for CH_4 formation are very consistent over the Pd/REO series, and have a value of 32 ± 1 kcal/mole. These values are again very close to that of 31.7 kcal/mole obtained for pure Pd powder. This result implies that the principal route for the methanation reaction is the same on all the

TABLE 5

Kinetic Behavior of Pd Catalysts for CO Hydrogenation (P = 14.6 atm, H_2/CO = 3)

Catalyst	Activity at 250°C (μmole · s^{-1} · g^{-1} × 10^3)			TOF at 250°C[a] (s^{-1} × 10^3)			E_a (kcal/mole)			% Selectivity (S) to oxygenates[b]		% Dimethyl ether in oxygenates at 250°C (carbon basis)
	CH_4	CO_2	CH_3OH	CH_4	CO_2	CH_3OH	CH_4	CO_2	CH_3OH	at 250°C	at 225°C	
1.50% Pd/La_2O_3	8.8	9.0	112	1.1	1.1	13.4	31.5	25.3	17.5	92.8	96.5	1
1.60% Pd/CeO_2	5.8	1.9	20.3	0.7	0.2	2.4	33.3	25.6	18.3	78.6	88.0	7
1.60% Pd/Pr_6O_{11}	5.1	3.3	64	0.5	0.3	6.0	35.6	32.1	18.8	93.4	96.7	12
1.55% Pd/Nd_2O_3	13.0	8.8	88	2.2	1.5	14.8	32.5	33.5	17.0	87.1	93.0	1
1.52% Pd/Sm_2O_3	10.7	9.1	123	0.7	0.6	7.5	34.6	25.4	17.6	92.0	95.6	1.5
1.66% Pd/Eu_2O_3	6.5	10.3	81	0.4	0.6	4.5	28.1	25.0	20.0	93.2	95.0	7
1.67% Pd/Gd_2O_3	3.4	3.5	83	0.3	0.2	6.8	32.8	24.6	20.7	96.2	98	3
Pd Powder	0.08	0.02	0.12	0.19	0.04	0.27	34.4	15.2	16.6	53[c]	58[c] at 240°C	16

[a] Based on H_2 chemisorption on the used catalyst.

[b] $S = \left[\frac{R_{CH_3OH} + 2R_{DME}}{R_{CH_3OH} + 2R_{DME} + R_{CH_4}}\right] \times 100$ where R is the rate.

[c] Considerable amounts of C_2H_6 formed, included in the calculation.

Pd/REO catalysts as well as the Pd powder. These results are somewhat higher than many values reported in the literature for other Pd catalysts; however, in this study, care was taken to stabilize the catalysts prior to the Arrhenius runs and they exhibited no loss of activity during these measurements. In contrast to the behavior of CH_4, the E_a values for CO_2 formation varied over a wide range. The lowest value (16.1 kcal/mole) was obtained for Pd powder, the highest value (28.1 kcal/mole) occurred over Pd/Gd_2O_3. This is presumed to be due to different pathways of CO_2 formation as a consequence of an interaction between CO and the REO support.

As can be seen from the last column of Table 4, all the Pd/REO catalysts produced detectable amounts of CH_3OH and DME at 1 atm pressure, but Pd powder did not. The ratio (R) of the TOF for CH_3OH to that of CH_4 at 225°C is presented in the table, and the ratio varies from 0.5 for Pd/CeO_2 to 2.8 for Pd/Eu_2O_3. This clearly shows that even at low pressures CH_3OH formation is kinetically favored over CH_4 formation on these Pd/REO catalysts although thermodynamic constraints limited overall conversion, and the CH_3OH formation at 1 atm pressure decreased with increasing temperature.

Table 5 presents the catalytic behavior of Pd/REO and Pd powder catalysts in the CO hydrogenation reaction at 14.6 atm. Listed are the activities at 250°C, turnover frequencies based on H_2 chemisorption on the used catalyst after the reaction, and the activation energies for the products CH_4, CO_2, and CH_3OH. The major product formed on all these catalysts at high pressure was CH_3OH, while CH_4, CO_2, and dimethyl ether were formed in smaller quantities. Over Pd powder, a considerable amount of C_2H_6 was also formed in addition to the above mentioned products. Also listed in the table are the selectivities, S, of these catalysts for oxygenate formation on

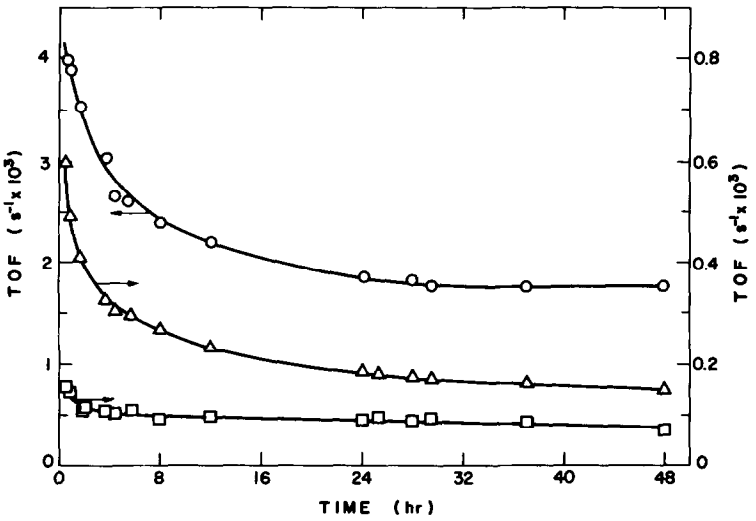

FIG. 3. Activity maintenance for 1.66% Pd/Eu_2O_3 at 14.6 atm and 225°C ($H_2/CO = 3$): CH_3OH (○); CH_4 (□); CO_2 (△).

a carbon atom basis. Since the only oxygenates formed over these catalysts were CH_3OH and DME, S can be calculated as

$$S = \left[\frac{N_{CH_3OH} + 2N_{DME}}{N_{CH_3OH} + 2N_{DME} + N_{CH_4} + 2N_{C_2H_6}}\right] \times 100,$$

where N could be either the turnover frequency or the activity for that particular product. The % DME in the total oxygenate product, calculated on a carbon basis, is also listed in Table 5 for each catalyst.

It can be noted in Table 5 that the activities of these Pd/REO catalysts for CH_4, CO_2, and CH_3OH formation varied over a small range. Pd/CeO_2 was the least active CH_3OH catalyst producing 20.3×10^{-9} mole $CH_3OH/s \cdot g$ cat. with a TOF of 2.4×10^{-3} s^{-1}. For all the Pd/REO catalysts, the activity of the catalysts for each product decreased rapidly with time in the initial stages of the reaction then dropped slowly. All the catalysts reached stable conversion levels after about 24 hr on-stream, but the reaction was normally monitored for 48 hr in order to ensure stable behavior, and the activity and turnover frequency values reported in Table 5 are the steady-state values reached after 48 hr on-stream. All activity maintenance curves were similar for the Pd/REO catalysts, and typical curves for CH_4, CH_3OH, and CO_2 are shown in Fig. 3 for Pd/Eu_2O_3. The fraction of synthesis activity remaining after achievement of stable catalytic behavior was about 0.4 for all the Pd/REO catalysts except for Pd/Eu_2O_3, for which it was about 0.5. The ratio of steady-state activity to initial activity in the case of CH_4 formation was found to vary between 0.4 and 0.6 within the series. Contrary to the Pd/REO catalysts, CH_3OH formation increased with time over the Pd powder catalyst and reached a steady-state rate in about 30 hr, while the CH_4 activity decreased initially for about 3 hr and then increased steadily, also approaching a steady-state value in 30 hr. The activity maintenance curves for CH_3OH and CH_4 on Pd powder in Fig. 4 show that the steady-state activity of CH_3OH was 1.9 times more than the initial activity and that of CH_4 was 1.3 times more than the initial activity. This may be due to further reduction of the large (1 μm) Pd crystallites under high-pressure reaction conditions, but it may also be a consequence of hydride formation and particle fracturing to increase

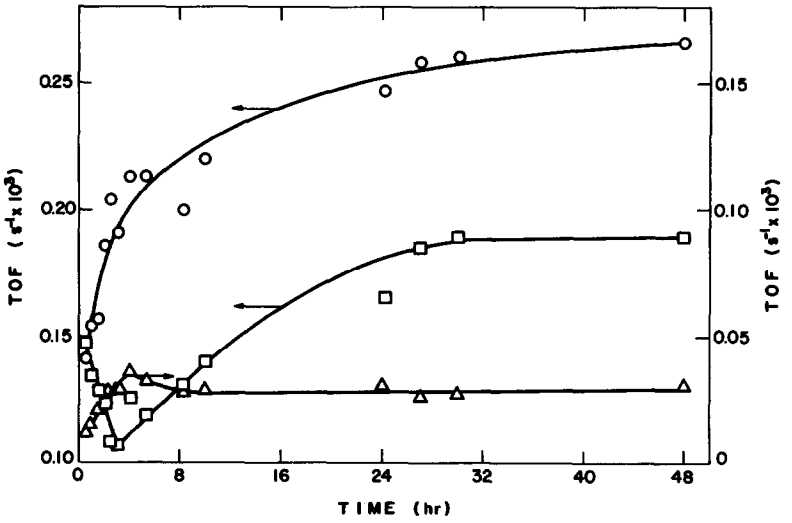

FIG. 4. Activity maintenance for Pd powder at 14.6 atm and 225°C ($H_2/CO = 3$): CH_3OH (○); CH_4 (□); DME (△).

surface area. Pd/Sm_2O_3 was found to be the most active catalyst producing 123×10^{-9} mole $CH_3OH/s \cdot g$ cat.; however, the highest TOF was obtained with the Pd/Nd_2O_3 sample. The Pd powder had very low activity compared to the Pd/REO catalysts due to its very poor dispersion. The TOF for CH_4 varied between 0.3×10^{-3} s^{-1} for Pd/Gd_2O_3 and 2.2×10^{-3} s^{-1} for Pd/Nd_2O_3, while the CH_3OH TOF varied between 2.4×10^{-3} s^{-1} for Pd/CeO_2 and 14.8×10^{-3} s^{-1} for Pd/Nd_2O_3. The corresponding values for Pd powder were 0.19×10^{-3} and 0.27×10^{-3} s^{-1}, respectively. Therefore, even after correcting for the poor dispersion, Pd powder was 10–50 times less active than the Pd/REO catalysts for CH_3OH production; however, the CH_4 TOF value was much more similar to values for the Pd/REO catalysts.

The activation energies for CH_4 formation at high pressure were quite similar to those obtained at 1 atm and they ranged from 31.5 to 35.6 kcal/mole, except for Pd/Eu_2O_3 which had a value of 28.1 kcal/mole. Unlike the behavior at 1 atm pressure, the Arrhenius plots for CO_2 formation at high pressure were straight lines for all the catalysts. This is attributed to the fact that the catalysts were on stream for a long time before the temperature effect was studied. Arrhenius plots for Pd/Nd_2O_3 and Pd powder are shown in Figs. 5 and 6. The E_a for

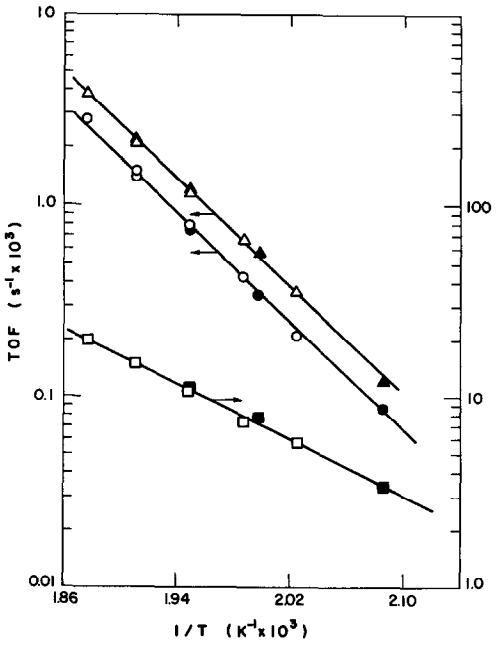

FIG. 5. Arrhenius plots for CH_3OH (△), CH_4 (□), and CO_2 (○) over 1.55% Pd/Nd_2O_3 ($P = 14.6$ atm, $H_2/CO = 3$). Open symbols, increasing T; filled symbols, decreasing T.

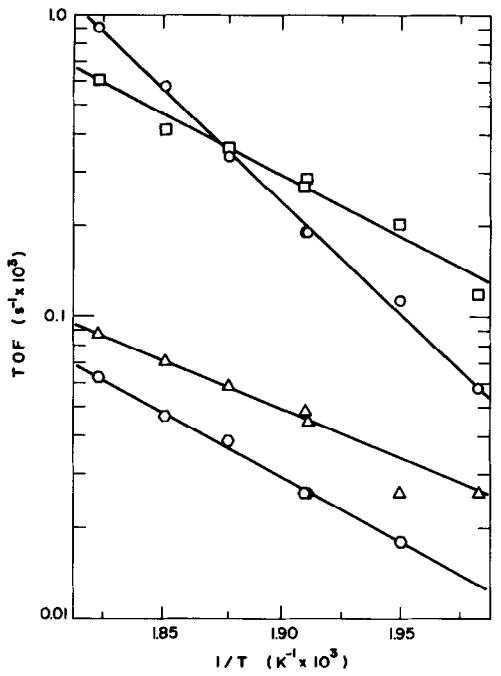

FIG. 6. Arrhenius plots over Pd powder (P = 14.6 atm, H_2/CO = 3). CH_3OH (□); CH_4 (○); DME (○), CO_2 (△).

CH_3OH formation varied over a narrow range of 17.0 kcal/mole for Pd/Nd_2O_3 to 20.7 kcal/mole for Pd/Gd_2O_3. For the Pd powder, the corresponding value was 16.6 kcal/mole. All these values, which are very similar, suggest that the rate determining step in CH_3OH formation involves similar surface intermediates. The E_a values for DME formation could be obtained only on certain catalysts because in some cases the quantities formed were too low to be properly quantified; however they ranged between 20 and 27 kcal/mole, in reasonable agreement with previous values (*7*).

It is clear from the data presented in Table 5 that the selectivity of all the Pd/REO catalysts for oxygenate formation is excellent at 14.6 atm, and the selectivity is slightly higher at 225°C compared to 250°C. Except for Pd/CeO_2, which has only 88% selectivity, all the catalysts were above 93% selectivity to oxygenates at 225°C. The amounts of DME in the total oxygenate product are also presented in Table 5, and they range from 1 to 12%. On Pd powder, the selectivity to oxygenates at 240°C was only 58%, of which 16% was DME, and this selectivity over unsupported Pd is somewhat lower than the value of 75% reported by Ryndin *et al.* (*7*) for Pd black. This is attributed to the somewhat different reaction conditions and to any alkali metal impurities that may be present in Pd (and Pt) blacks, which can increase selectivity and activity of supported Pd catalysts for CH_3OH and reduce E_a values for the reaction (*8*).

DISCUSSION

Differences exist among various authors regarding the principal factors which govern methanol formation from syngas over supported Pd catalysts. In the first report on this subject, Poutsma *et al.* suggested that the ability of Pd to catalyze methanol formation was due to its excellent hydrogenation ability coupled with its inherent tendency to adsorb CO nondissociatively even at reaction temperatures, and that adsorbed CH_xO species were intermediates (*5, 25*). Ryndin *et al.* found that basic supports generally favored CH_3OH formation and that dimethyl ether could be formed by a secondary reaction occurring on acid sites on the support (*7*). Fajula *et al.* concluded that weak CO chemisorption on small Pd crystallites favored selectivity to CH_3OH and that the presence of different Pd hydride phases might alter catalytic behavior (*6*). Ponec and co-workers have argued that partially oxidized Pd species (Pd^{n+}) are responsible for CH_3OH synthesis (*9, 10, 26*), although Fajula *et al.* detected no partially oxidized Pd using XPS (*6*). More recent studies have provided results both consistent (*27, 28*) and inconsistent (*8, 29, 30*) with the presence of Pd^{n+} species.

Various CH_xO_y species on supported Pd catalysts, such as formyl (–CHO), formate (–COOH), and methoxy ($-OCH_3$) groups, have been detected by IR spectroscopy and

chemical trapping methods (*8, 11, 28, 31, 32*). Naito *et al.* correlated CH_3OH activity with adsorbed formate species (*31*), while Hindermann *et al.* observed a relationship between activity and formyl species (*28*). The lack of detection of such groups on unpromoted Pd/SiO_2 catalysts was a consistent result in these studies. These previous results have shown that methanol formation from syngas is sensitive to both the support and promoters like alkali metals, and low CH_3OH activities exist over La_2O_3, CeO_2, and ThO_2 in the absence of a metal whereas SiO_2, MgO, and Al_2O_3 are essentially inactive (*33*). A variety of reaction paths involving CH_xO_y species formed on the support have been proposed (*33–39*), including one involving H_2 spillover onto the support to hydrogenate these species to form CH_3OH (*33*).

From this study (Table 5), we know that Pd metal by itself is capable of producing both CH_4 and CH_3OH from syngas, but the activity again is very low. However, the combination of Pd with any of these REO supports greatly enhances the activity for CH_3OH formation while CH_4 formation at higher pressure is affected to a much smaller extent. This indicates that there is a synergistic effect involved. Since both CH_4 and CH_3OH are formed on Pd powder, where the Pd crystallite size is extremely large, it is possible that there are two pathways for the formation of CH_4 on Pd catalysts: one via disproportionation of CO on particular Pd sites which may be favored on small crystallites as suggested by Boudart and co-workers (*40–42*) and others (*9*), and the other via decomposition of an oxygen-containing intermediate (*43*). However, the activation energy values for CH_4 formation on all the Pd/REO catalysts studied in our work (Tables 4 and 5) at both 1 and 14.6 atm are very close to the corresponding values obtained for pure Pd powder, and this may indicate that on all our catalysts CH_4 was forming through a common intermediate, which we believe at this time is very likely to be surface carbon formed from CO dissociation on certain types of Pd sites. It is difficult to believe that significant quantities of Pd^{n+} species could exist on the pure Pd powder because of its extremely large particle size and the high H_2 pressures used, yet it forms CH_3OH with reasonably high selectivity. Consequently, we are inclined to discount the role of Pd^{n+} in CH_3OH formation.

One extremely interesting result is apparent from a comparison of the CH_4 TOF values at 523 K at both 1 and 14.6 atm, which are listed in Tables 4 and 5. The specific activity for CH_4 showed little increase, and in some cases declined, as the pressure increased nearly 15-fold. Only the Pd powder exhibited a significant (six-fold) rate enhancement. This was unexpected as the pressure dependence for methanation has typically been found to range between $\frac{1}{2}$ to 1 (*6, 22*), which would predict rate increases from 4 to 15. The CH_4 activation energies are nearly identical at both pressures, implying no change in the mechanism; consequently, one conclusion is that some of the *active* sites for methanation on the supported catalysts have been lost, or converted to CH_3OH active sites, at higher pressure. The shift from the α- to the β-hydride phase through this pressure region may be a partial explanation (*6*).

We believe it is possible that there are also two routes for CH_3OH formation from CO and H_2 on Pd catalysts, as suggested by Kiennemann and co-workers (*37–39*). The first is through formate intermediates involving the support and the second is through formyl intermediates existing primarily on the Pd. On Pd/SiO_2, Pd/C, and Pd powder, only the second route exists because no additional surface oxygen is available for the formation of the formate species. On other catalysts like Pd/La_2O_3, Pd/CeO_2, and Pd/Al_2O_3, both mechanisms may operate. This is proposed from the observation that no formate species were detected on Pd/SiO_2, that the activities of Pd/La_2O_3, Pd/ThO_2, and Pd/Al_2O_3 were not influenced by the presence of alkali ions on the surface, and that the activities of Pd/

SiO_2 and Pd/C catalysts were similar. It is evident from Table 5 that the TOF value for CH_3OH formation on the Pd powder is very low compared to those on supported Pd catalysts, including Pd/SiO_2 (*12*). This may indicate that even on catalysts where only the formyl route operates, enhancements due to the support can still occur. At this time, the exact manner in which the support influences the reaction is not known, but it is attributed to an interaction of a formyl intermediate with the support surface and these sites are most likely to exist at the Pd–support interface.

Since both formyl and formate species were detected on Pd/La_2O_3 and Pd/N_2O_3 (*28*) and since the rare earth oxides have similar chemical properties, we have assumed that the CH_3OH synthesis reaction can proceed through either intermediate on Pd/REO catalysts. Formyl species can form on either the Pd surface or on the support surface, as suggested by others (*34, 35*), and formate-like species can form by the migration of the formyl species from Pd to the support surface (*31, 32*), or by the insertion of CO into –OH groups on the support (*28, 33, 36–39*). Both species can be hydrogenated to $-OCH_3$ species and finally to CH_3OH (*37–39, 44*). Since the activation energies for CH_3OH formation on all the Pd/REO catalysts studied were similar (17.0–20.7 kcal/mole), which is close to the value of 16.6 kcal/mole on the Pd powder, and since the existence of formate species on the Pd powder is not likely, it seems reasonable to conclude that the slow step may be similar in these catalysts; for example, the addition of hydrogen to the C=O bond in either of these surface species. This would allow the interconversion between formyl and formate species on the supported catalysts.

Regarding the formation of DME, we cannot reach any definite conclusions from our data, but it seems that the less basic the REO, the higher the DME formation (Table 5), which is in agreement with Ryndin *et al.* (*7*). Although the relationship between support acidity and DME formation may be valid, it does not explain the considerable formation of DME on pure Pd powder. Consequently, it may be possible to form DME by a route other than dehydration on the support, such as a reaction of one of the intermediates in the formation of CH_4, such as $-CH_2$ or $-CH_3$, with one of the intermediates in the formation of CH_3OH, such as $-OCH_3$ or $-CH_2O$. This is consistent with the more equal CH_4 and CH_3OH synthesis rates on pure Pd.

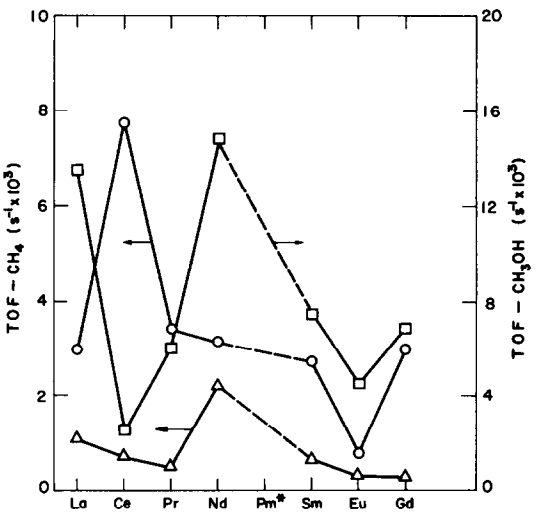

FIG. 7. Effect of RE oxide on CH_4 and CH_3OH turnover frequencies. CH_4 at 1 atm, 548 K (○); CH_4 at 14.6 atm, 523 K (△); CH_3OH at 14.6 atm, 523 K (□).

The relationship between the TOF values at both 1 and 14.6 atm and the atomic number of the RE element is shown in Fig. 7. For CH_4 formation at 1 atm, a sharp peak occurs with Ce and a minimum exists with Eu, whereas at 14.6 atm the pattern of CH_4 specific activity is decidedly different and the range of TOF values is much narrower; that is, the ratio of the most active to the least active is 13 at 1 atm and 4 at 14.6 atm. For CH_3OH formation there is a minimum rate using Ce and a sharp maximum at Nd followed by a gradual decrease thereafter. The pattern for the CH_3OH TOF's is very reminiscent of that reported by Ichikawa and Shikakura for Pt dispersed on a variety of supports with different electronegatives (e.g., basicities) (*44*).

It is significant to note that the CH_4 rate dependence at 1 atm, shown in Fig. 7, is very similar to the dependence of the CO_2 yield in the total oxidation of butane on these rare earth oxides, as reported by Hattori *et al.* (*45*). They found that the oxidation activity was directly proportional to the ease of oxidation of the +3 state to the +4 state, i.e., it was inversely proportional to the fourth ionization potential of the rare earth atom. Evidence strongly indicates that C–O bond dissociation of the adsorbed surface species—whether it is CO or an H_xCO intermediate—is the rate-determining step in the methanation reaction on Pt and Pd (*22, 24, 43*). Under our reaction conditions, which are strongly reducing, more than one oxidation state for the rare earth ions may exist on the support surface near the Pd crystallites. It has been suggested by some workers that support cations or oxygen vacancies which are adjacent to the metal crystallites can exert some influence on the adsorption of CO or on the dissociation of the C–O bond in CO or $-CH_xO$ species adsorbed on the supported metal (*24, 29, 46*). This interaction can be depicted as

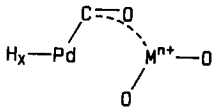

where M is a metal ion. Comparing the relationship between the CH_4 TOF and the atomic number of the RE element (Fig. 7) with the activity dependence of Hattori *et al.* (*45*), we propose that the specific activity on these REO catalysts may be related to a redox cycle associated with a change in valence of the RE cation, for example, with the transformation of a +3 ion to a +4 ion. Thus, Pd/CeO_2 is the most active *methanation* catalyst because of Ce^{3+} can be oxidized to Ce^{4+} most easily and so the interaction shown above is maximum when M^{n+} is Ce^{3+}. The minimum activity of Pd/Eu_2O_3 may be because it is the most easily reduced and M^{n+} in this case is most likely Eu^{2+} rather than Eu^{3+} (*47*), and, due to the larger size of the Eu^{2+} ion and its stability, this interaction may be noticeably reduced. These active sites are presumed to exist predominantly at the metal–support interface, i.e., interface sites, which allows for facile reduction to the lower valent state by hydrogen dissociated on the Pd. A more complete study of Pd dispersed on all the REOs further supports this proposal (*48*). The most important conclusion here is that the support itself plays a major and direct role in the catalytic sequence of steps which produces CH_4. This was observed previously using experimental procedures which enhanced interface contact between Pd and the REO support (*17*).

The catalytic activity for CH_3OH may also correlate with the resistance of the trivalent RE ion to oxidize to the tetravalent ion, a property which should be indirectly related to the basicity of the RE oxide support used. The ease of migration of the –CHO (formyl) species from the Pd surface to the oxide surface depends on the ability of the RE oxide oxygen to accept the formyl species, which in turn depends on the Lewis basicity of the oxide. A similar trend was observed in the hydrogenation of ethylene on these oxides (*49*), which might indicate that the hydrogenating ability of these rare earth oxides also plays a role in the determination of CH_3OH synthesis activity of the Pd/REO catalysts, perhaps through the hydrogenation of the formate species on the oxide surface.

SUMMARY

This investigation has demonstrated that REO-supported Pd provides very good CO hydrogenation catalysts. At atmospheric pressure and low temperature, the major product was methanol but the selectivity shifts to methane at higher temperatures because of equilibrium constraints. The TOF values for CH_4 are an order of magnitude higher on these catalysts compared to Pd/SiO_2 or pure Pd metal and they are similar to those reported for Pd/Al_2O_3 or Pd/SiO_2–Al_2O_3. The activation energies for

CH_4 on all these catalysts varied over a very narrow range and were very close to the value on Pd powder, indicating that the methanation reaction mechanism may be similar on all these catalysts, including large, unsupported Pd crystallites. Significant amounts of CO_2 were formed over the supported Pd systems, but the activation energy for its formation varied noticeably. A relationship between the CH_4 TOF at 1 atm and the ease of oxidation of the trivalent rare earth ion to the tetravalent one appears to exist which strongly indicates that the support cations at the metal-support interface are directly involved in the catalytic sequence. Depending on the ease of the redox cycle between valence states, such as between the +3 ion and the +4 ion, these RE oxides may aid in the breaking of C–O bonds of adsorbed CO or $-CH_xO$ species, which is the rate-determining step in the methanation reaction.

At 14.6 atm total pressure, the major product over all the Pd/REO catalysts was methanol, and the selectivity for oxygenates ranged from 78 to 96% at 225°C. The activation energies for CH_3OH on these catalysts varied between 17 and 20 kcal/mole and were close to the value obtained for Pd powder. Pd/La_2O_3 and Pd/Nd_2O_3 were the most active CH_3OH catalysts with TOF's of 13–15 $\times$ 10^{-3} s^{-1} whereas Pd/CeO_2 was the least active with a TOF value of 2.4 $\times$ 10^{-3} s^{-1}. All the Pd/REO catalysts deactivated initially at high pressure, but reached steady state after about 30 hr on stream, with the stabilized activity being approximately half the initial activity for all these Pd/REO catalysts. The activity of Pd powder increased with time and reached a steady state. The selectivity of Pd powder for oxygenates was lower (58% at 240°C) compared to the Pd/REO catalysts, and the CH_3OH TOF over Pd powder was an order of magnitude smaller than the least active supported Pd catalyst. The role of the support in CH_3OH synthesis is consistent with that of increasing the concentration of formyl/formate intermediates on the surface, particularly at the Pd–support interface.

ACKNOWLEDGMENT

This study was supported by a grant from Koppers, Inc.

REFERENCES

1. Meisel, S. L., McCullough, J. P., Lechthaler, C. H., and Weisz, P. B., *CHEMTECH* **6,** 86 (1976).
2. Anderson, E. V., *Chem. Eng. News,* July 16, 1984.
3. Kung, H. H., *Catal. Rev.-Sci. Eng.* **22,** 235 (1980).
4. Klier, K., "Advances in Catalysis," Vol. 31, p. 243. Academic Press, New York, 1982.
5. Poutsma, M. L., Elek, L. F., Ibarbia, P. A., Risch, A. P., and Rabo, J. A., *J. Catal.* **52,** 157 (1978).
6. Fajula, F., Anthony, R. G., and Lunsford, J. H., *J. Catal.* **73,** 237 (1982).
7. Ryndin, Yu. A., Hicks, R. F., and Bell, A. T., *J. Catal.* **70,** 287 (1981).
8. Kikuzono, Y., Kagami, S., Naito, S., Onishi, T., and Tamaru, K., *J. Chem. Soc. Faraday Discuss.* **72,** 135 (1981).
9. Poels, E. K., van Broekhoven, E. H., van Barneveld, W. A. A., and Ponec, V., *React. Kinet. Catal. Lett.* **18,** 223 (1981).
10. Driessen, J. M., Poels, E. K., Hindermann, J. P., and Ponec, V., *J. Catal.* **82,** 26, (1983).
11. Kikuzono, Y., Kagami, S., Naito, S., Onishi, T., and Tamaru, K., *Chem. Lett.,* 1249 (1981).
12. Berube, M. N., M. S. thesis. The Pennsylvania State University, 1984.
13. Kaiser, S. W., E.P. 0 031 244 and E.P. 0 031 243, assigned to the British Petroleum Company (1984).
14. Joyner, R. W., McCarroll, J. J., and Tennison, S. R., E.P. 101 645, assigned to the British Petroleum Company (1984).
15. Ichikawa, M., *J. Chem. Soc. Chem. Commun.,* 566 (1978).
16. Ichikawa, M., *Bull. Chem. Soc. Jpn.* **51,** 2268 (1978).
17. Mitchell, M. D., and Vannice, M. A., *Ind. Eng. Chem. Fundam.* **23,** 88 (1984).
18. Sudhakar, C., and Vannice, M. A., *Appl. Catal.,* **14,** 47 (1985).
19. Palmer, M. B., Jr., and Vannice, M. A., *J. Chem. Technol. Biotechnol.* **30,** 205 (1980).
20. Benson, J. E., Hwang, H. S., and Boudart, M., *J. Catal.* **30,** 146 (1973).
21. Yates, D. J. C., and Sinfelt, J. H., *J. Catal.* **8,** 348 (1967).
22. (a) Wang, S. Y., Moon, S. H. and Vannice M. A., *J. Catal.* **71,** 167 (1981); (b) Vannice, M. A., *J. Catal.* **37,** 449 (1975).
23. Berube, M. N., and Vannice, M. A., unpublished results.
24. Vannice, M. A., and Sudhakar, C., *J. Phys. Chem.* **88,** 2429 (1984).

25. Rabo, J. A., Risch, A. P., and Poutsma, M. L., *J. Catal.* **53,** 295 (1978).
26. Poels, E. K., Koolstra, R. B., Geus, J., and Ponec, V., *in* "Metal-Support and Metal-Additive Effects in Catalysis" (B. Imelik *et al.*, Eds.), p. 233. Elsevier, Amsterdam (1982).
27. Yoshioka, H., Naito, S., and Tamaru, K., *Chem. Lett.*, 981 (1983).
28. Hindermann, J. P., Kiennemann, A., Chakor-Alami, A., and Kieffer, R., *in* "Proceedings, 8th International Congress on Catalysis, Berlin, 1984," p. II-163.
29. Bracey, J. D., and Burch, R., *J. Catal.* **86,** 384 (1984).
30. Deligianni, H., Mieville, R. L., and Peri, J. B., Preprints, ACS Meeting, Philadelphia, Div. of Fuel Chem., p. 243 (1984).
31. Naito, S., Yoshioka, H., Orita, H., and Tamaru, K., *in* "Proceedings, 8th International Congress on Catalysis, Berlin, 1984," p. III-207.
32. Palazov, A., Kadinov, G., Bonev, Ch., and Shopov, D., *J. Catal.* **74,** 44 (1982).
33. Meriaudeau, P., Dufaux, M., and Naccache, C., *in* "Proceedings, 8th International Congress on Catalysis, Berlin, 1984," p. II-185.
34. Hattori, H., and Wang, G., *in* "Proceedings, 8th International Congress on Catalysis, Berlin, 1984," p. III-219.
35. Wang, G., and Hattori, H., *J. Chem. Soc. Faraday Trans. 1* **80,** 1039 (1984).
36. He, M. Y., and Ekerdt, J. G., *J. Catal.* **87,** 381 (1984).
37. Ramaroson, E., Kieffer, R., and Kiennemann, A., *J. Chem. Phys.* **79,** 759 (1982).
38. Ramaroson, E., Kieffer, R., and Kiennemann, A., *J. Chem. Soc. Chem. Commun.*, 645 (1982).
39. Hindermann, J. P., Deluzarche, A., Kieffer, R., and Kiennemann, A., *Canad. J. Chem. Eng.* **61,** 21 (1983).
40. Ichikawa, S., Poppa, H., and Boudart, M., *in* "ACS Symposium Series 248" (T. E. Whyte *et al.*, Eds.), Amer. Chem. Soc., p. 439. Washington, D.C. (1984).
41. Doering, D. L., Poppa, H., and Dickinson, J. T., *J. Catal.* **73,** 104 (1982).
42. Boudart, M., and McDonald, M. A., *J. Phys. Chem.* **88,** 2185 (1984).
43. Mori, T., Masuda, H., Imai, H., Miyamoto, A., Hasabe, R., and Murakami, Y., *J. Phys. Chem.* **87,** 3648 (1983).
44. Ichikawa, M., and Shikakura, K., *in* "Proceedings, 7th International Congress on Catalysis, Tokyo, 1980," p. 925.
45. Hattori, T., Inoko, J. I., and Murakami, Y., *J. Catal.* **42,** 60 (1976).
46. Ichikawa, M., *CHEMTECH*, 674 (1982).
47. Rosynek, M. P., *Catal. Rev.-Sci. Eng.* **16,** 111 (1977).
48. Vannice, M. A., and Sudhakar, C., to be published.
49. Khodakov, Yu. S., Nakshunov, V. S., and Minachev, Kh. M., *Kinet. Katal.* **12,** 535 (1971).